

The Data-Acquisition System with Cluster-Finding Trigger at the J-PARC KOTO Experiment

C Lin¹, Y B Hsiung¹, Y W Wah², Y C Tung², Y T Luo², and M Bogdan²

¹ Department of Physics, National Taiwan University, Taipei, Taiwan 10617, Republic of China

² Enrico Fermi Institute, University of Chicago, Chicago, IL 60637, USA

E-mail: jay@hep1.phys.ntu.edu.tw

Abstract. In order to collect the events efficiently with a high intensity beam, we built a new trigger electronics system based on the calibrated energy information and the number of electromagnetic shower clusters in the calorimeter for the J-PARC KOTO experiment. The dead time of this system is 0.16 μ s and the loss was measured to be less than 1%. By performing the online clustering algorithm on the simulated data, the trigger efficiency for the primary mode $K_L \rightarrow \pi^0 \nu \bar{\nu}$ is estimated to be 99.6%.

1. The KOTO Experiment

The J-PARC KOTO experiment aims to search for the rare kaon decay $K_L^0 \rightarrow \pi^0 \nu \bar{\nu}$, which is a CP-violating Flavor-Changing-Neutral-Current process. The decay is highly-suppressed in the standard model (SM) and sensitive to new physics because of the small theoretical uncertainty [1]. The signature of $K_L^0 \rightarrow \pi^0 \nu \bar{\nu}$ is two photon clusters in the calorimeter from the pion without any hits in other detector components, as shown in Fig. 1.

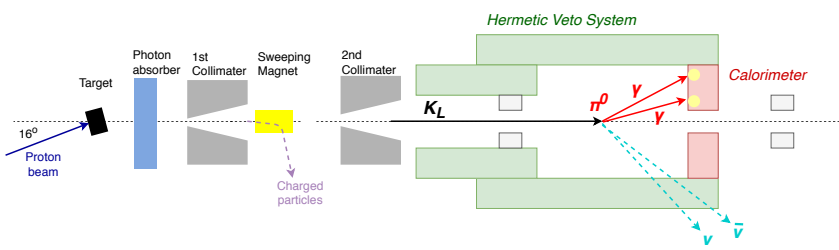


Figure 1. The KOTO detector. The CSI calorimeter is in red and the vetoes are in green.

2. The Data-Acquisition System

Figure 2 illustrates the architecture of the KOTO data-acquisition (DAQ) system. The pipeline readout is utilized to make the two-level trigger decisions. The level 1 (Lv1) trigger is determined by the combination of the total energy in the calorimeter (E_t) and veto bits from other detector components. The level 2 (Lv2) trigger is determined by the number of electromagnetic shower clusters in the calorimeter.



Content from this work may be used under the terms of the [Creative Commons Attribution 3.0 licence](#). Any further distribution of this work must maintain attribution to the author(s) and the title of the work, journal citation and DOI.

2.1. Lv1 Trigger System

At first, the custom-designed analog-to-digital converter (ADC) continuously samples the pulses from around 4000 channels every 8 ns. For the CSI crates, the Et is calculated by summing up the peak height in series. For the veto crates, the veto bit is set High when the peak height exceeds the threshold in each module. All the information is collected in the Local Clock Distribution and Trigger module (CDT). The Optical Fiber Center module (OFC) [2] receives 11 Et values and 7 sets of veto bits. The Et is summed up over 11 CSI inputs and the veto bits are obtained by taking OR of 7 veto inputs. Both final Et and veto bits are delivered to the Top CDT for the Lv1 trigger decision.

2.2. Lv2 Trigger System

A cluster trigger is issued if the Lv1 trigger is fulfilled. When the ADCs in the CSI crates receive the cluster trigger, a cluster bit is made from each channel based on the peak height. These bits are sent to the Clustering OFC. The cluster-finding is then performed according to a high-speed algorithm suggested by [3]. The dead time is 0.16 μ s and the data loss is less than 1%. The number will be reported to the Top CDT for the Lv2 trigger decision. In the end, the accepted trigger is distributed to all the ADCs if the event satisfies all the requirements. The corresponding waveforms are written out from the ADCs to the PC farm for event-building.

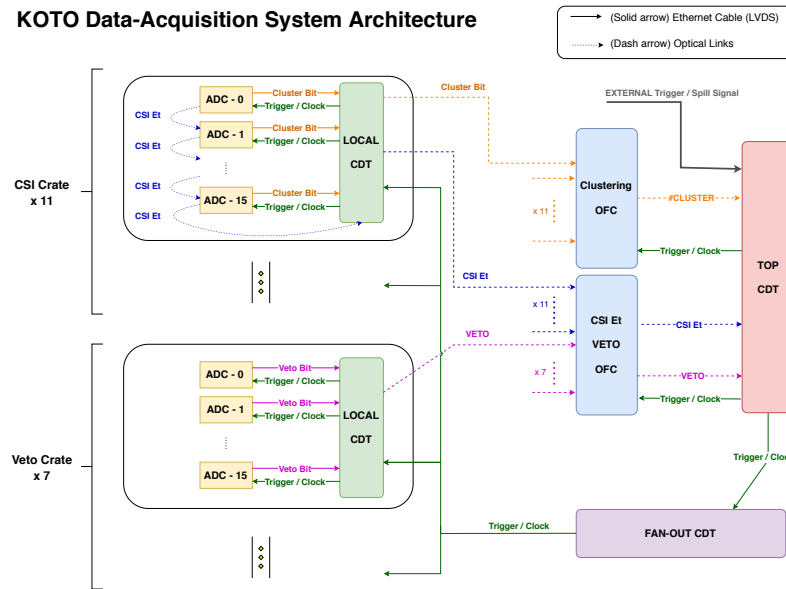


Figure 2. The simplified block diagram for the Et/veto and cluster trigger.

3. Performance

3.1. Lv1 Trigger

The data triggered by Et was used to check the Lv1 trigger performance. The offline Et distribution was fitted with an exponential function and the ratio of the data point to the fitted value was defined as the efficiency for the Et trigger as shown in Fig. 3. For the vetoes, the online veto decision was tagged through the data and the efficiency was obtained as shown in Fig. 4. Both plots are fitted by the error functions and the offline threshold are about 3σ away from μ , indicating a little loss from the Lv1 trigger.

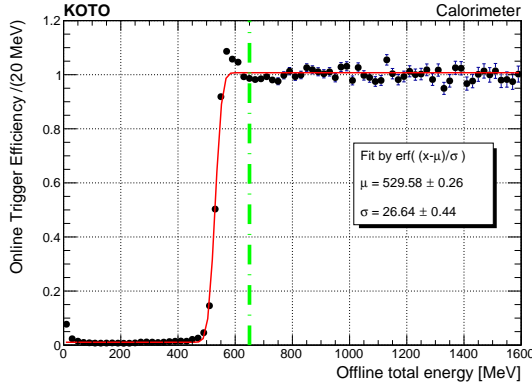


Figure 3. The efficiency versus the offline total energy under online Et trigger. The green line indicates the total energy cut for $K_L^0 \rightarrow \pi^0 \nu \bar{\nu}$. The black dots show the efficiency at each energy bin. The red line represents the fitted result.

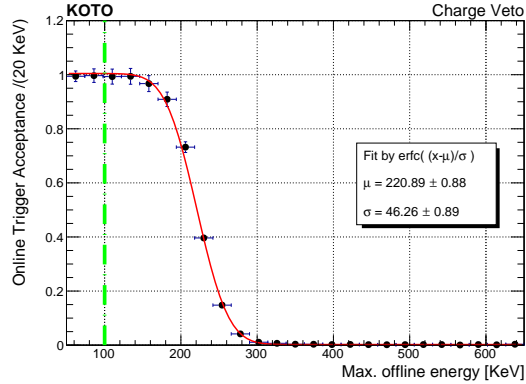


Figure 4. The acceptance versus the maximum offline energy among all the channels with online veto. The green line indicates the veto threshold for $K_L^0 \rightarrow \pi^0 \nu \bar{\nu}$. The black dots show the efficiency at each energy bin. The red line represents the fitted result.

3.2. Lv2 Trigger

To extrapolate the efficiency for the $K_L^0 \rightarrow \pi^0 \nu \bar{\nu}$ events, the online clustering effect was simulated with a GEANT4-based Monte Carlo (MC) simulation. The algorithm was applied to the simulated pulses and the same selection criteria was applied for the data. Table 1 shows the efficiency for both data and MC. The trigger efficiencies are in good agreement, and the efficiency for the primary mode $K_L^0 \rightarrow \pi^0 \nu \bar{\nu}$ was estimated to be 99.6%.

Table 1. The trigger efficiency of data (ϵ_{data}) and Monte Carlo simulation (ϵ_{mc})

Mode	ϵ_{data} [%]	ϵ_{mc} [%]
$K_L^0 \rightarrow \pi^0 \pi^0$	96.8	96.7
$K_L^0 \rightarrow 2\gamma$	99.6	99.2
$K_L^0 \rightarrow \pi^0 \nu \bar{\nu}$	—	99.6

4. Conclusion

The new DAQ system with the cluster-counting trigger was commissioned in June 2018 for the KOTO experiment. It has a small dead time of 0.16 μ s and less than 1% data loss. Moreover, the online trigger has the high efficiency of 99.6% for the $K_L^0 \rightarrow \pi^0 \nu \bar{\nu}$ collection and this effect was well simulated by Monte Carlo simulation.

References

- [1] Buras A J, Buttazzo D, Girrbach-Noe J and Knegjens R 2015 *Journal of High Energy Physics* **2015** 33
- [2] Bogdan M, Lin C, Luo Y, Tung Y and Wah Y 2019 *Nucl. Instrum. Methods Phys. Res.* **936** 340 – 341
- [3] Haney M J, Gollin G D and Yamanaka T 1992 *IEEE Conference on Nuclear Science Symposium and Medical Imaging* 338–340 vol.1